Sze, Eric H.Y.; Koo, Raymond C.H.; Leung, Jojo M.Y. and Ho Ken K.S. (2018) Design of Flexible Barriers against Sizeable Landslides in Hong Kong. HKIE Transactions, Vol. 25, No. 2, pp. 115-128.

The Assessment Board selected this paper for the 2020 HKIE Geotechnical Paper Award, for its potential to advance local geotechnical practice and its quality of writing for the readership of practicing geotechnical engineers. It hence noted.

The paper critically reviewed the world-wide design practices of channelized debris flow flexible steel barrier and reported on a Hong Kong case where such valley-shaped barriers were designed for construction, incorporating some innovative features. This is one of the pilot projects in designing a valley-shaped flexible steel barrier in Hong Kong using the pseudo dynamic impact force approach for construction, and the first time the design methodology and considerations were reported in details in the public domain. The design methodology was adequately discussed and justified for practitioners to follow and to judge for its reliability. The paper was well written complete with useful photographs and illustrations. The paper also made insightful suggestions on areas for further improvements. The design methodology may be adopted for future design in Hong Kong and provides a strong basis for the future development of a flexible steel barrier Design Code for Hong Kong.

This is an **Accepted Manuscript** of an article published by Taylor & Francis in **HKIE Transactions** on 2018, available online at the Taylor & Francis Ltd web site: www.tandfonline.com (Link to the article: https://doi.org/10.1080/1023697X.2018.1462107)

# Design of flexible barriers against sizeable landslides in Hong Kong

**Eric H Y Sze, Raymond C H Koo, Jojo M Y Leung & Ken K S Ho**

Pages 115-128 | Received 19 Dec 2017, Accepted 03 Apr 2018, Published online: 31 Jul 2018

## ABSTRACT

A new type of flexible debris-resisting barrier has been designed using the state-of-the-art analytical force approach for mitigation of channelised debris flow hazards in a hillside study area in Hong Kong. Unlike the conventional three-panel rectangular form, these flexible barriers were configured in a valley shape to geometrically fit in the incised drainage lines. The "design event" resulted in a calculated debris impact pressure of up to 400 kPa and over 10,000 kJ in terms of impact energy necessitating a site-specific design. The design involved advanced structural modelling of the highly non-linear behaviour of flexible barriers under debris impact giving rise to a large deformation. This paper presents the design and detailing of these valley-shaped flexible barriers, involving formulation of the design methodology, derivation of the multi-phase impact load model and optimisation of the barrier configuration. To support the design, numerical parametric studies were conducted to examine the barrier's impact behaviour. Two design initiatives were highlighted for enhancing the design robustness, including a rigorous approach to analyse the effects of the energy-dissipating devices on barrier performance and a robustness check to cater for adverse scenarios that could conceivably happen. Some suggestions on configuring a valley-shaped flexible barrier were given.

KEYWORDS: Flexible barrier, natural terrain landslides, drainage line, design, force approach, Hong Kong

## 1. Introduction

### 1.1. Characteristics of flexible debris-resisting barriers

Over the last decade, steel flexible barriers are emerging as a promising structural counter-measure to mitigate landslide and debris flow hazards [1–3]. When subjected to debris impacts, flexible barriers deflect and allow the debris to travel with the steel net for a certain distance. This results in significant dissipation of the impact energy due to strain energy development in the barrier and internal energy losses within the decelerating debris. From the force and momentum transfer perspective, such debris–barrier interaction effectively prolongs the impact process and hence attenuates the impact load exerted on the barrier. To achieve this mechanism, the barrier is typically equipped with a layer of interception net that is supported by wire ropes and spanned by posts on a hinged base. Energy-

dissipating devices are commonly installed along the ropes to enhance the energy absorption capacity. The ropes and posts are all anchored to the ground.

So far, almost all flexible barriers installed in Hong Kong are proprietary rockfall protection kits with an energy rating certified by the European Organisation for Technical Approvals (EOTA) [4]. The structural form of these barriers is standardised in the form of a three-panel rectangular system (Figure 1(a)). Due to its less restrained structure, the barrier can undergo large deformation locally to effectively arrest high-velocity rockfall [5]. A similar form has also been used to resist shallow landslide impact from an open hillside taking advantage of its wide areal coverage [6]. The use of these prescribed barriers to mitigate channelised debris flow (CDF) that takes place in an incised drainage line would unavoidably alter its geometry, rendering it less structurally effective and less cost effective. An example is shown in Figure 1(b). The side panels are redundant in terms of intercepting the debris flow. In this case, a valley-shaped barrier that better fits the channel geometry would be preferred, such as those described by Roth et al. [7] and Volkwein et al. [8]. However, such valley barriers have not yet been adopted in Hong Kong.

Figure 1. Examples of proprietary rockfall-resisting flexible barriers in Hong Kong installed: (a) on an open hillside; and (b) in an incised drainage line.


### 1.2. Design practice in Hong Kong

The design of flexible debris-resisting barriers in Hong Kong commonly follows either the empirical approach [9] or the energy approach [10]. Both methods specify an energy requirement based on which a certified proprietary rockfall barrier is proposed by the designer and procured by the contractor. A major drawback of these methods is that the design debris-resisting capacity of the barrier is relatively limited. For example, for the flexible barrier with the highest certified energy rating (8600 kJ) nowadays, its design energy dissipation capacity is 6450 kJ (a scaling factor of 0.75 is applied pursuant to the Geotechnical Engineering Office (GEO) [9]). This roughly corresponds to 100 $m^3$ debris travelling at 7.5 m/s, or 200 $m^3$ at 5.5 m/s.

More sizeable events thus call for an alternative scheme. Reinforced concrete rigid barriers are usually favoured since the design and construction requirements are more routine in nature even though the works can cause environmental concerns and are unsightly. Steel flexible barrier designed using the analytical force approach is another feasible option. Such a design method is novel and not yet well developed for flexible debris-resisting barriers [8,10]. This approach is less favoured by the local practitioners mainly because of

the perceived complexity involved in the design process, the need to undertake non-routine numerical modelling and the difficulties in configuring the barrier layout, etc. The cause of the above perceptions is probably an inadequate understanding of both the implementation of the design approach and the impact behaviour of flexible barriers.

Ng et al. [11] were the first to adopt the force approach in Hong Kong for design of flexible barriers to resist debris impact arising from an open hillslope failure. Chan et al. [12] also presented a design of a framed flexible barrier system with an energy rating of 5040 kJ. Both of these barriers were in a conventional rectangular form akin to the proprietary rockfall barriers. Also, these projects only specified a single type of energy-dissipating device for the flexible barrier. This means that the barrier would not perform as intended if the specified type of energy-dissipating device is not used. That could limit the choice of product suppliers in the tendering process and may elevate the construction cost.

### 1.3. This study

Recently, four out of seven flexible debris-resisting barriers were designed based on the analytical force approach, as works under the Landslip Prevention and Mitigation Programme (LPMitP) administered by the GEO for a hillside study area in Hong Kong. The design was undertaken by the GEO with structural design input provided by the Architectural Services Department, the HKSAR Government. These flexible barriers were mainly targeted at sizeable landslides with an estimated debris impact pressure up to 400 kPa and an impact energy loading over 10,000 kJ. Three of these flexible barriers were specifically designed to be in a trapezoidal geometry in order to fit in the incised drainage lines. These barriers were considered geometrically more favourable and structurally more effective in resisting CDF corresponding to a significant design event taking place along a drainage channel.

This paper presents the development of these valley-shaped flexible barriers, which are the first of this kind in Hong Kong. The design was based on advanced numerical modelling to analyse the behaviour upon debris impact on the barriers under the multi-phase non-uniform load application. Parametric studies were conducted to examine the effects of varying the barrier configuration, including energy-dissipating device specification and wire rope layout. To avoid mimicking a specific type of energy-dissipating device, a new design approach was proposed to analyse more rigorously the design limit states of the barrier. This was done by modelling the force-elongation characteristic of the energy-dissipating device, using a set of lower and upper bound design curves. In addition, in order to enhance the design robustness, a performance check was undertaken to review the barrier responses under certain possible adverse scenarios (e.g. malfunctioning of some of the energy-dissipating devices). In this paper, the implementation of the force approach for design of flexible debris-resisting barriers is elaborated. Based on this study, some suggestions on configuring an optimised barrier layout for the use in a drainage line or incised topography are provided. The findings serve as a reference for practitioners who intend to carry out similar design, analysis and detailing in practice.

## 2. Project background

The study area (about 6 ha in area and 100 m in elevation difference) is located at Kwai Chung flanking Castle Peak Road (Figure 2). It comprises 11 hillside catchments, three of which contain incised drainage lines with perennial stream flow. According to the natural terrain hazard study (NTHS), six catchments were found to be posing undue landslide risk to the downslope facilities, including some cottages and the carriageways, pursuant to the react-to-known-hazard principle [13]. Potential landslide hazards in each vulnerable catchment were identified, as shown in Figure 2. The estimated design debris volumes (i.e. the design events) are also shown. The estimation was based largely on the largest recent landslides that took place in 1997 and 2008 within the study area. Together with the predicted entrainment volume for CDF, the largest design event was found to be 260 $m^3$.

Figure 2. Natural terrain study area with catchment classification, potential landslide hazards, their design events and predicted debris runout paths as well as the proposed locations of flexible barriers.

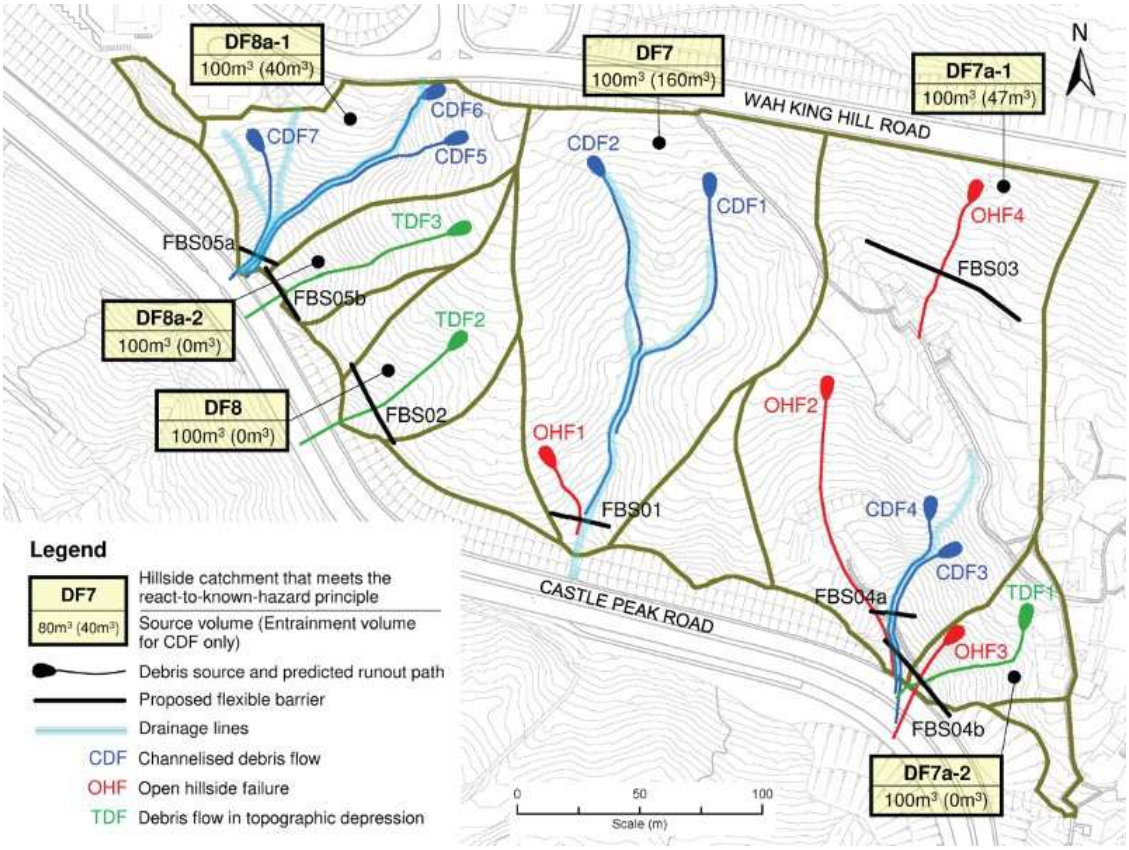


To mitigate these landslide hazards, flexible debris-resisting barriers were selected as a cost-effective and sustainable scheme based on a detailed design option assessment. In choosing the optimal barrier location, due considerations were given to the envisaged debris flow paths, the debris mobility (which affects the impact loading), the buildability of the barriers and their effects on the surroundings (e.g. slope stability, trees), etc. Debris mobility simulation was carried out by numerical modelling [14] using the recommended

rheological parameters given by GEO [15–17]. Figure 2 shows the predicted debris runout paths and the proposed locations of the flexible barriers.

The results of debris mobility modelling were used to establish the design impact loading, in terms of impact energy loading ($E$) and dynamic impact pressure ($P_d$), based on Equations (1) and (2), respectively, pursuant to Kwan and Cheung [10]. For the estimation of $P_d$, the hydrodynamic pressure coefficient ($\alpha$) was taken as 2.0. This $\alpha$ value is considered appropriate for the design of flexible barrier under debris impact in Hong Kong, based on a review by Kwan and Cheung [10]. Also, based on the NTHS for this study area, the debris flow event was not envisaged to contain boulders of diameter over 2 m, so a higher $\alpha$ value to account for the effects of large hard inclusions was not required. Table 1 summarises the design debris flow velocity and flow depth, as well as the debris impact energy and impact pressure calculated at each barrier location.

$$E = \min[\max(E_{k1}, E_{k2}), \max(E_p, E_r)] \text{ , (1)}$$

where $E_{k1}$ = kinetic energy of the whole debris mass when the debris front reaches the barrier location; $E_{k2}$ = kinetic energy of the debris mass that passes the barrier location; and $E_p$, $E_r$ = impact energy of the debris assuming the pile-up and run-up mechanisms [18], respectively.

$$P_d = \alpha \rho_d v^2 \text{ , (2)}$$

where $\rho_d$ = density of moving debris, taken conservatively as 2200 kg/m$^3$; and $v$ = design debris flow velocity (m/s).

**Table 1. Results of debris mobility modelling and evaluation of debris impact loadings.**

| | | | | Design parameters at barrier locations | | | |
|---|---|---|---|---|---|---|---|
| **Hillside catchments** | **Critical landslide hazards** | **Proposed flexible barriers** | **Design approach adopted[a]** | **Flow velocity, *v* (m/s)** | **Flow depth, *h* (m)** | **Impact energy, *E* (kJ)** | **Impact pressure, $P_d$ (kPa)** |
| DF7 | OHF1 | FBS01 | Force | 4.0 | 0.6 | 534 | 70 |
| DF8 | TDF2 | FBS02 | Energy | 8.0 | 0.6 | 5,577 | 282 |
| DF7a-1 (upper hillside) | OHF4 | FBS03 | Empirical | Not required | | | |
| DF7a-1 (lower hillside) | CDF4 | FBS04a | Force | 9.5 | 1.0 | 6,956 | 397 |
| DF7a-2 | TDF1 | FBS04b | Force | 9.0 | 0.6 | 6,901 | 356 |
| DF8a-1 | CDF7 | FBS05a | Force | 9.3 | 0.6 | 11,191 | 381 |
| DF8a-2 | TDF3 | FBS05b | Energy | 8.8 | 0.6 | 5,464 | 341 |

The adopted design approach for each flexible barrier is also shown in Table 1. Amongst the seven flexible barriers, four of them were designed based on the analytical force approach. For FBS04a, 04b and 05a, since they were subjected to an excessively calculated energy loading, they had to be designed using the force approach in lieu of the energy approach. Apart from the technical feasibility, it should be emphasised that the decision on opting for a viable design approach was also made with due regard to the cost effectiveness of the works. For example, given the low energy demand on FBS01, a 1000 kJ proprietary rockfall barrier could have been readily assigned as the design solution [9]. However, it was still designed as a valley-shaped barrier that better fits the channel geometry using the force approach because of the envisaged material and cost savings, as illustrated in Figure 3.

Figure 3. Illustration of the difference between a valley-shaped flexible barrier and the conventional three-panel rectangular system.

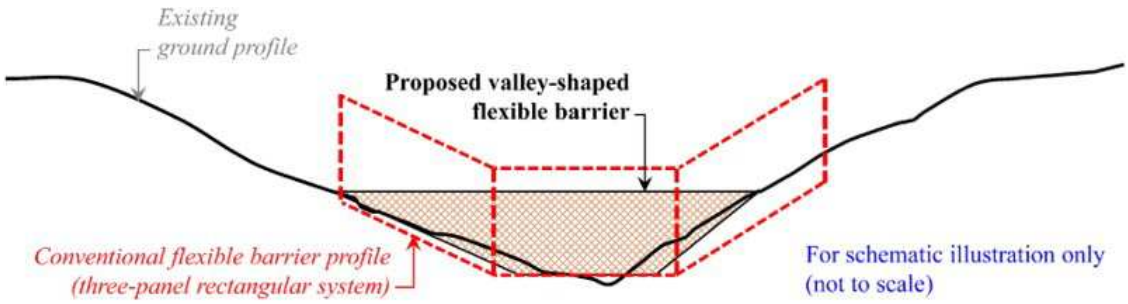


## 3. Formulation of the design framework using force approach

### 3.1. General design framework

In this study, the step-by-step procedures for designing a flexible debris-resisting barrier based on the force approach have been formulated following the principle outlined by Kwan and Cheung [10], as shown in Figure 4. It broadly comprises the following four key stages:

1. Initial setup

   This stage involves establishing the design impact scenarios and configuring the flexible barrier before combining them for analysis. The impact scenarios, based on the multi-phase load model, comprise sequential application of dynamic impact load (Equation (2)) and static earth load due to debris deposition (assuming an earth pressure coefficient of 1.0) in multiple phases. The barrier has to be configured in terms of its position, size, netting arrangement, layering of wire ropes and specification of energy-dissipating devices to achieve adequate debris-resisting capacity against the design events. To achieve an optimised barrier layout, iterations with the next stages are required to review the impact behaviour of the barrier and update its configuration accordingly.

2. Design and analysis

   To analyse the performance of the flexible barrier under the design impact scenarios, numerical soil–structure interaction analysis is required because of the highly non-linear geometrical and material stress–strain behaviour of the structure. Computer programmes that have been used in practice include FARO [19], NIDA-MNN [20] and LS-DYNA [11]. The simulation results provide data for detailed structural design of the members and foundations in accordance with the relevant codes of practice. The barrier deformation profiles are also computed in the numerical analysis for checking of the retention capacity. Depending on the utilisation of these capacities, the barrier configuration could be optimised.

3. Robustness check

   This is an additional stage introduced in this study to ensure the robustness of the design under some adverse but plausible scenarios that could affect the barrier performance. Examples include malfunctioning of energy-dissipating devices, debris overtopping the barrier and asymmetrical load application. This check is primarily safety-oriented, and hence the overall design objective is to avoid the collapse of the structure.

4. Detailing and specification

   Examples of detailing are the connections between wire ropes and the ground/ steel net/ posts, the anchoring system and their corrosion protection specifications. Measures to enhance the design robustness may be included, e.g. abrasive protection devices for the top wire ropes [21]. Discussion of this design stage (Stage 4) is outside the scope of this paper.

Figure 4. Adopted design framework based on the analytical force approach.

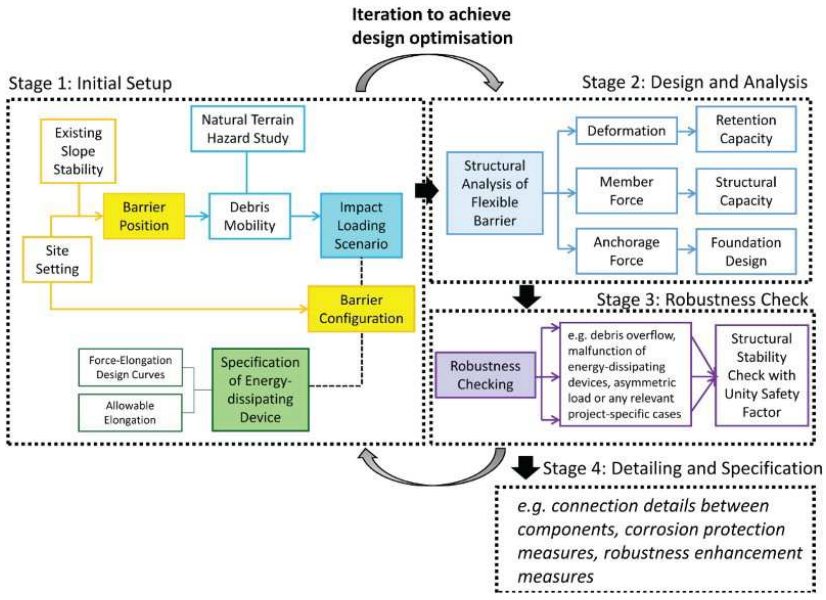

### 3.2. Design requirements

Apart from the generic design requirements suggested by Kwan and Cheung [10], several other specific requirements have been considered in this project, as listed below.

1. The flexible barrier was designed as a non-sacrificial barrier.

2. None of the energy-dissipating devices was over-utilised, i.e. utilisation ratio (UR) $\leq 100\%$.

$$UR = \frac{\delta}{\delta_{allow}} \times 100\%, \quad (3)$$

where $\delta$ = mobilised elongation of an energy-dissipating device; and $\delta_{allow}$ = allowable elongation of the same energy-dissipating device

3. No debris overflow was allowed, i.e. all debris was retained by the flexible barrier.

## 4. Development of valley-shaped flexible barriers

The flexible barriers FBS01, 04a and 05a were positioned within the three drainage lines in the study area in order to resist the CDF impact. Since the drainage lines are incised, a rational configuration for these barriers would be in the form of a trapezoidal shape such that they could better fit into the channels (e.g. Figure 3 as an example). The use of a conventional three-panel system in such a site setting renders its side panels less effective. Also, especially for an incised topography, a valley-shaped barrier, as compared with the conventional barrier, would require less substantial site formation works, which are both costly and environmentally unfriendly to undertake in a natural hillside setting. Another merit of this alternative structural form is that the wire ropes can be directly anchored to the sides of the channel, thereby providing extra restraint that is required to resist the areal loading of debris flow [22].

In the following sections, the development of the valley-shaped flexible barriers, based on the above-formulated design framework, is presented. The design of FBS04a, which was subject to the largest impact loading, is discussed. Results of parametric studies are also highlighted to enhance understanding of the impact behaviour of this valley barrier.

### 4.1. Proposed configuration of FBS04a

The optimised configuration of FBS04a is shown in Figure 5. The flexible barrier was laid symmetrically within the drainage line in a location that could intercept all envisaged debris flow paths. The overall barrier size was controlled by its retention capacity. Its basic configuration comprised bottom, top and border wire ropes on the four sides to hold the steel net in the place within the channel. The winglet rope was provided to offer additional vertical restraint and confine the flow of any overtopping debris in order to avoid eroding the channel sides. Two layers of middle ropes were added at the lower portion of the barrier, where the impact was envisaged to be the greatest. All these longitudinal support ropes

were anchored directly to the sides of the drainage line. Steel posts on hinged bases were provided to support the top ropes because of its large lateral span. The posts were tied to the back slope by two pairs of retain ropes, which further enhanced the debris-resisting capacity of the flexible barrier. Energy-dissipating devices were provided in each rope.

Figure 5. Optimised configuration of a valley-shaped flexible barrier (FBS04a) proposed in this project.

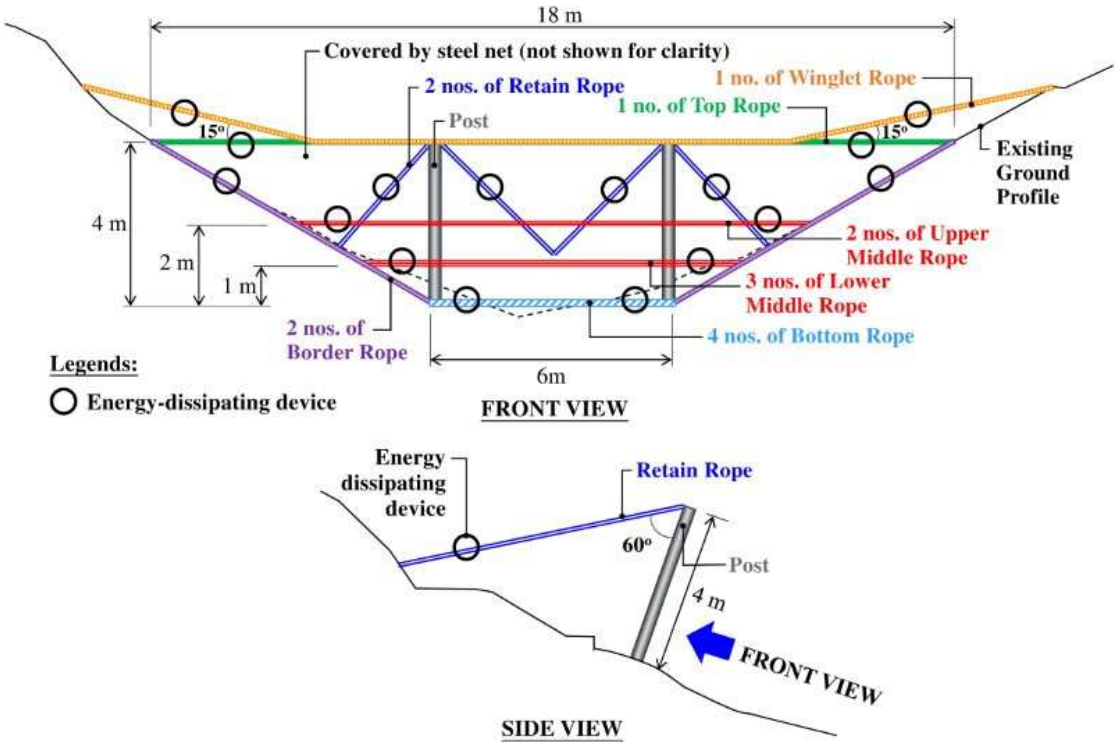


## 4.2. Specifications of energy-dissipating devices

Unlike previous projects, the flexible barriers in this study were not designed specifically to a certain product of energy-dissipating device. Figure 6 shows the lower and upper bound characteristic design curves for the energy-dissipating devices proposed for FBS04a, which encompassed several proprietary product curves. The approach was to design for the limiting barrier responses based on these bounding curves so that the barrier would perform as intended no matter which type of energy-dissipating device is adopted for the construction, provided that their characteristic curves fall within the design bounds. In addition, this would cater for some deviation or variability in the behaviour of the as-built energy-dissipating devices.

Figure 6. Proposed lower and upper bound characteristic design curves for the energy-dissipating devices together with examples of curves of the selected proprietary products.

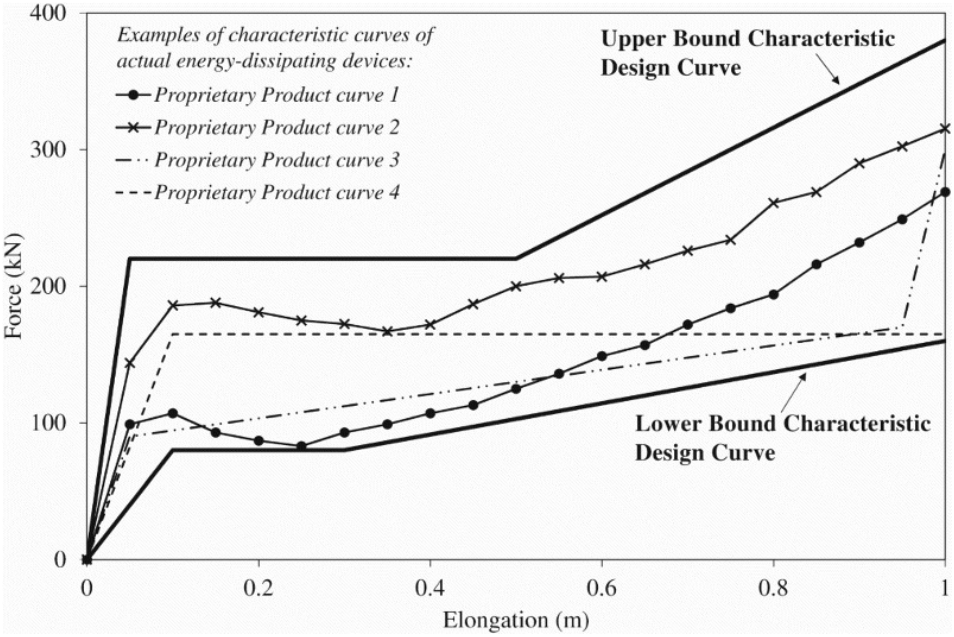


In essence, the force-elongation curve controls the stiffness of a wire rope and the allowable elongation ($\delta_{allow}$) of the energy-dissipating device. Since the lower bound curve represents the most ductile behaviour with the least energy absorption capacity, it is critical to the barrier deformation behaviour. On the other hand, the upper bound curve represents the stiffest behaviour and is thus critical to the forces induced in the structure. Apart from these bounds, another design requirement for an energy-dissipating device was to specify its $\delta_{allow}$. Following the same principle as discussed above, a lower bound value of 1 m and an upper bound value of 4 m have been considered in the design. This bound was assigned with reference to the actual allowable elongation of proprietary products of energy-dissipating devices commonly used in practice. If the device elongates beyond δallow, the rope would behave in accordance with its own mechanical stiffness.

### 4.3. Impact-loading scenarios

Based on debris mobility modelling by DAN [14] using the rheological parameters for CDF as recommended by GEO [15] based on systematic back analyses of good-quality local case studies (i.e. an apparent friction angle $\varphi_a = 11°$, a turbulence coefficient $\xi = 500$ m/s$^2$ in a Voellmy model), the design flow velocity and depth at the location of FBS04a were found to be 9.5 m/s and 1.0 m, respectively (Table 1).

Following the procedures suggested in GEO [23], the number of debris impact load phases acting on the flexible barrier was determined. By considering a first phase of impact by 1.0 m thick debris flow ramping at an angle of 10° flowing to the barrier and based on the site topography, the volume of the first debris flow phase was estimated (about 20 m$^3$). Following the same principle, the volume of the second phase riding on top of the first one

was also determined (about 75 $m^3$). Given a design event of 147 $m^3$, it could be deduced that a total of three impact load phases would be acting on the flexible barrier, as shown schematically in Figure 7.

Figure 7. Design impact loading scenarios based on the multi-phase load model.

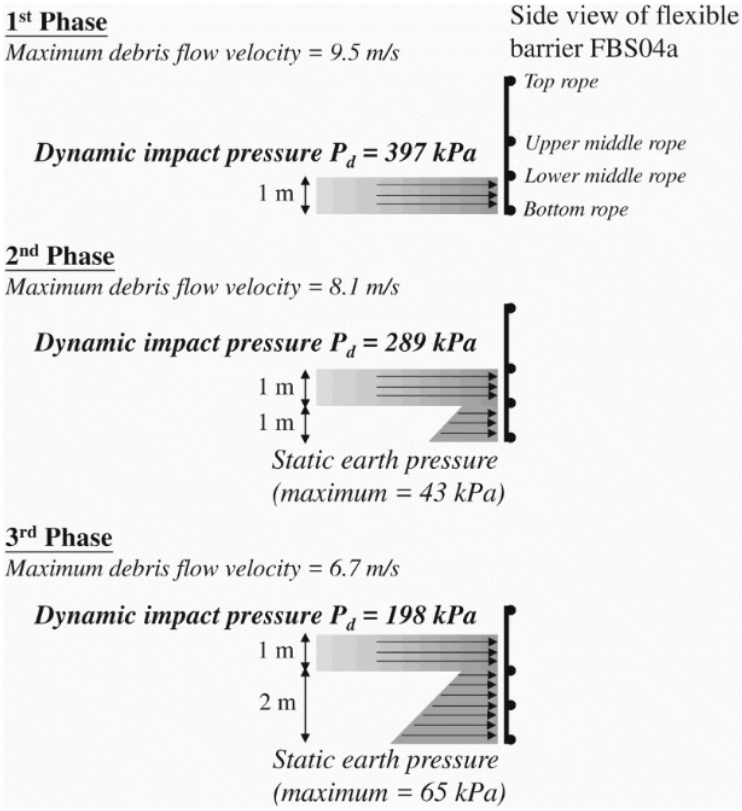


Using Equation (2) and taking into account the effects of debris velocity attenuation as proposed by Koo et al. [24], the calculated dynamic impact pressure ($P_d$) was about 400 kPa in the first phase and subsequently reduced to about 200 kPa in the last phase. $P_d$ was assumed to be uniform across the width of the barrier in each phase of debris impact. The static earth pressure varied with the debris height. Since the debris would sit on the net once it is arrested, the effect of its self-weight needed to be accounted for in the analysis.

### 4.4. Analysis of the impact behaviour

In this study, a non-linear finite-element programmes NIDA-MNN, was used to analyse the impact behaviour of the flexible barriers. This programme is suitable for simulating the highly non-linear behaviour of a flexible structure that undergoes large deformation under loading. Chan et al. [20] discussed several essential features of this programme that are relevant to flexible barrier modelling. For example, it adopts “sliding node” elements to model the “curtain effect” of a steel net sliding on a wire rope as well as “non-linear cable” elements to replicate the non-linearity of an energy-dissipating device. This programme

has been used by Kwan et al. [3] to back-analyse a local case of landslide that impacted on a flexible barrier.

### 4.4.1. Verification of the numerical programme

Wendeler et al. [2] reported a series of field tests involving actual debris flows impacting on instrumented flexible barriers installed in the Illgraben catchment of Switzerland. As more comprehensive data were reported, the event that took place on 18 May 2006 was selected for verification of NIDA-MNN in this study. In this event, a large amount (15,000 $m^3$) of debris flowing with a frontal velocity of 2.9 m/s filled up and overtopped a flexible barrier that spanned across a channel.

The numerical model and the assumed impact loading scenarios are shown in Figure 8. Based on the findings by Huang et al. [25], who back-analysed this event using a fully coupled model LS-DYNA, the debris impact pressure was computed as 70 kPa. Table 2 compares the simulated and measured maximum axial forces for the bottom and top ropes. It was found that NIDA-MNN, based on the multi-phase impact load model, was able to capture rope forces similar to the reported field measurements. It only over-estimated the bottom rope force by about 10%. The fact that the top rope force was over-predicted by almost 30%, was probably because the effect of the debris velocity attenuation [24] was not considered in the simulation. The results were also comparable with that predicted by FARO [26], which has been used routinely by a supplier for the design of its proprietary flexible barriers, and LS-DYNA [25], which was based on a fully coupled analysis with explicit modelling of the debris–barrier interaction.

Figure 8. Verification of NIDA-MNN against the Illgraben field test: (a) the simulated flexible barrier; (b) the assumed impact loading scenario; and (c) comparison of simulated and observed barrier deformation after impact [2].

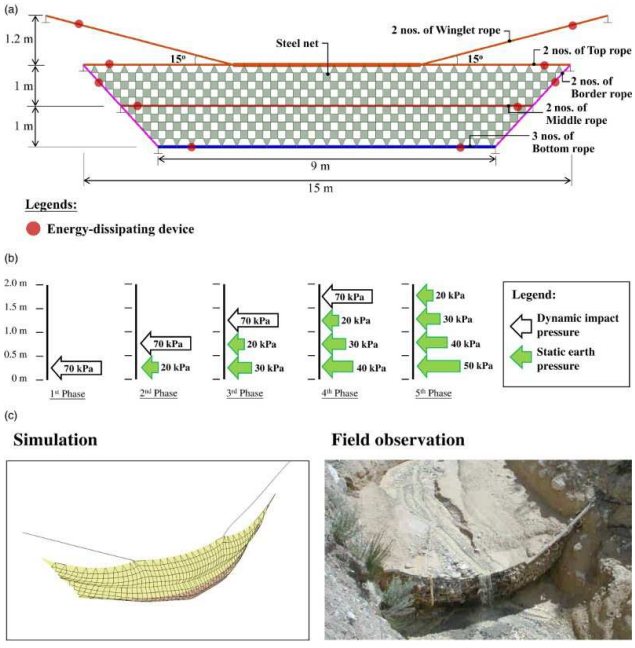

Table 2. Comparison of the simulation results and field measurements for verification of NIDA-MNN.

| | Field measurements by Wendeler etal. [2] | Simulation by NIDA-MNN (this study) | Simulation by FARO (Bartelt etal. [26]) | Simulation by LS-DYNA (Huang etal. [25]) |
|---|---|---|---|---|
| Maximum bottom rope force (kN) | 248 | 279 | 240 | 261 |
| Maximum top rope force (kN) | 150 | 196 | 170 | 200 |

### 4.4.2. Impact behaviour of the flexible barrier

The same modelling technique of NIDA-MNN has been applied to analyse the impact behaviour of FBS04a. Figure 9 shows the numerical models adopted in NIDA-MNN, which explicitly replicated the proposed barrier configuration (Figure 5). As discussed above, the analyses were carried out for both lower and upper bound characteristic design curves of energy-dissipating devices. Figure 10 compares the computed barrier deformation profiles in each impact phase for both the lower and upper bound cases. As can be seen from the figure, the flexible barrier responded to each impact phase with a large deflection, which peaked at the centre. The conversion of dynamic impact load to static earth load resulted in a retraction of the net because of the corresponding load reduction. Evidently, the barrier deformed more significantly in the lower bound case. Bulging of the net was the largest in the first load phase, where the impact pressure was the highest, giving rise to about 3.3 m forward deflection (1 m more than the upper bound case). The net also sagged more, such that the top rope dropped vertically by about 1.0 m (0.4 m more than the upper bound case).

Figure 9. Numerical model of FBS04a in NIDA-MNN.

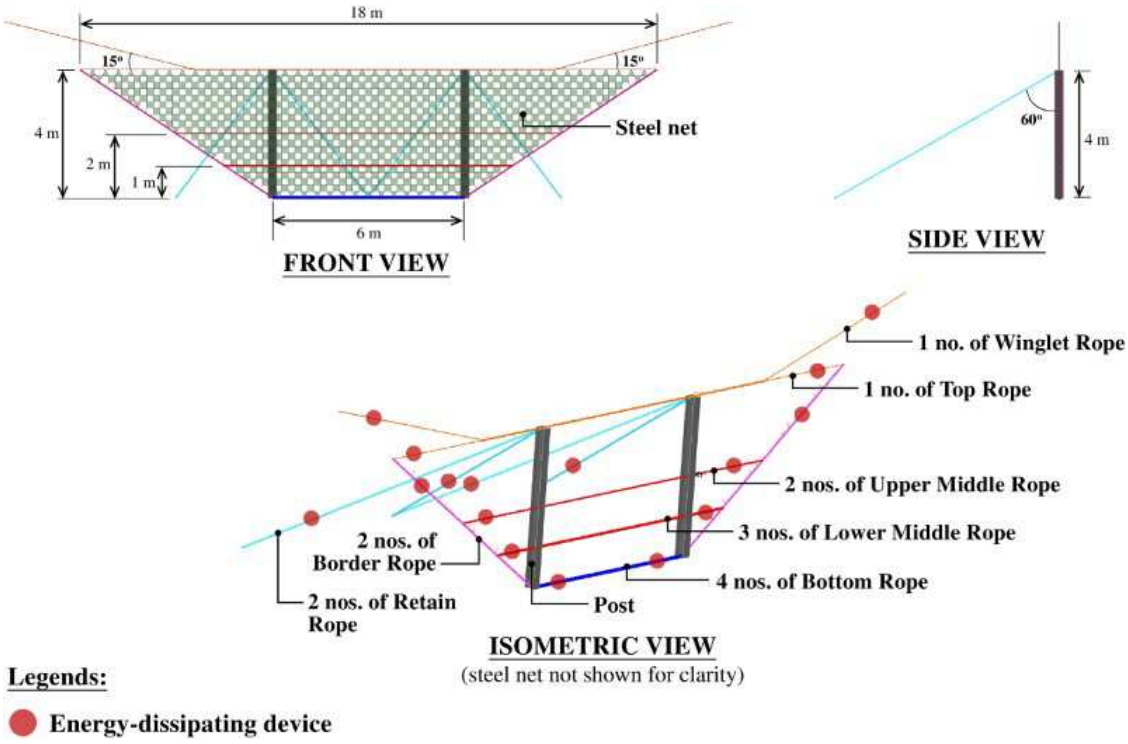


Figure 10. Comparison of the impact behaviours of FBS04a designed based on the lower bound and the upper bound characteristic design curves of energy-dissipating devices.

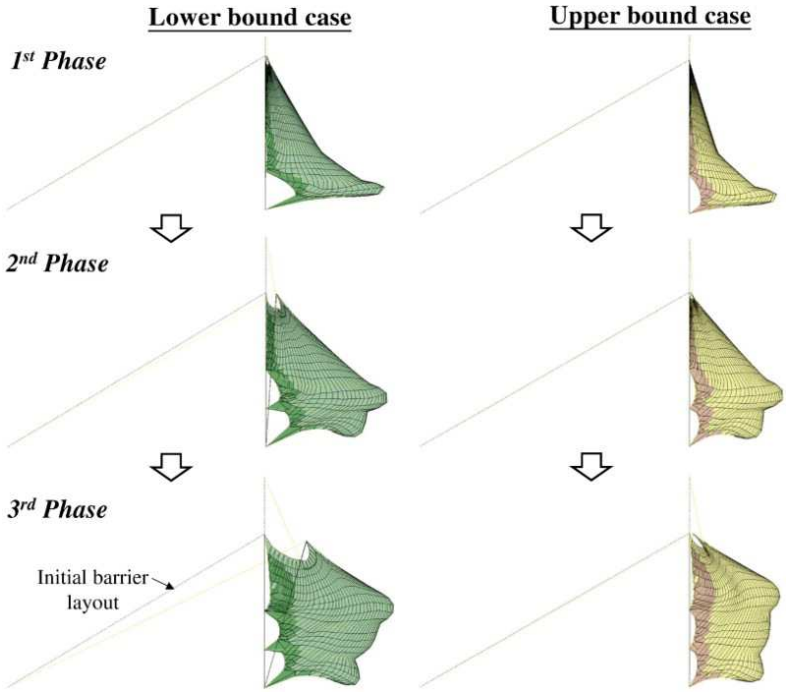

The larger barrier deformation in the lower bound case was attributed to the greater mobilisation of the energy-dissipating devices, which can be reflected in their utilisation ratio (UR, Equation (3)) as plotted in Figure 11(a) for each group of the wire ropes. The maximum UR ranged from 70% to 100% in the lower bound case as compared with 5% to 45% in the upper bound case. As the main impact took place at the lower portion of the barrier, the energy-dissipating devices of the corresponding wire ropes (i.e. bottom, lower middle and border ropes) were almost fully mobilised in the first load phase. For other ropes in the upper portion, their UR gradually built up as the impact load shifted upward in the subsequent load phases. It was of interest to note that the retain ropes could only be utilised when all other energy-dissipating devices were significantly mobilised. This was because the bulged barrier was being pushed to lean forward due to successive exertions of impact loading. The corresponding mobilised rope forces are compared in Figure 11(b). As the rope force development was controlled by the characteristic design curves, the upper bound case resulted in a higher cable force (up to 220 kN). The drop of axial forces in some wire ropes was attributed to the relaxation of their energy-dissipating devices due to the unloading phase after each debris impact.

Figure 11. Comparison of the results of structural modelling of FBS04a between the lower and upper bound cases: (a) the utilisation ratio of energy-dissipating devices; and (b) the axial forces mobilised in different groups of wire ropes.

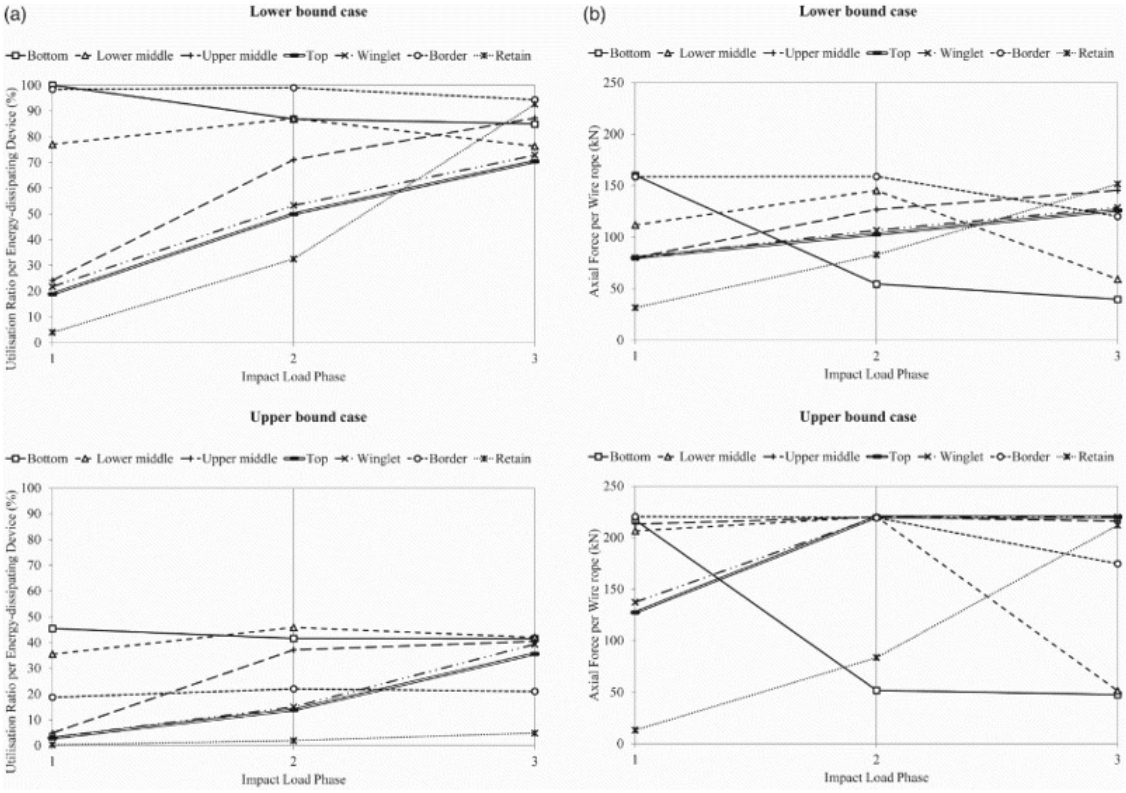


Table 3 compares the results of structural modelling for FBS04a associated with different specifications of energy-dissipating devices, i.e. lower bound, upper bound, a product curve that falls within the bounds (Figure 6) and the case with no such devices at all. Based

on the results, the beneficial effects of equipping energy-dissipating devices in a flexible barrier were revealed. The mobilised rope forces would be increased substantially if such devices were not provided. The barrier would also behave in a stiffer manner with limited deformation. On the other hand, it can be observed that the design limits of the barrier were successfully captured with the use of the proposed bounding curves. The results using the actual product curve fell well within these design limits. In this case, the utilisation ratios of all energy-dissipating devices were high (mostly well over 65%) suggesting that the designed configuration for FBS04a was essentially optimised.

Table 3. Comparison of the results of structural modelling for FBS04a with different specifications of energy-dissipating devices.

| | **Maximum axial force per rope (kN)[utilisation ratio shown in bracket]** | | | |
|---|---|---|---|---|
| **Wire rope** | **Lower bound curve** | **Upper bound curve** | **Proprietary product curve 1[a]** | **No energy-dissipating device** |
| Bottom | 160 [100%] | 217 [45%] | 188 [75%] | 575 [-] |
| Lower middle | 145 [87%] | 220 [46%] | 174 [67%] | 676 [-] |
| Upper middle | 146 [87%] | 220 [40%] | 173 [67%] | 681 [-] |
| Top | 126 [70%] | 220 [36%] | 146 [56%] | 413 [-] |
| Winglet | 129 [73%] | 220 [39%] | 151 [59%] | 378 [-] |
| Border | 159 [99%] | 220 [22%] | 169 [66%] | 238 [-] |
| Retain | 152 [93%] | 212 [5%] | 162 [64%] | 135 [-] |
| Maximum deformation of flexible barrier (m) | | | | |
| Bulging of net | 3.5 | 2.3 | 3.1 | 1.7 |
| Sagging of top rope | 1.0 | 0.6 | 0.9 | 0.4 |

## 4.5. Robustness checking

To enhance the design robustness, an additional performance check was proposed in this study to examine the flexible barrier responses under certain adverse scenarios. Table 4 lists three robustness check scenarios specifically considered for FBS04a and the underlying rationale. It should be noted that these scenarios, amongst other possible assumptions, were selected for assessment in this design project only. They serve to illustrate the concept of robustness checking and how it could be applied in practical design. The choice of the credible adverse scenarios to be considered in the robustness check is based primarily on the judgement and may be different for other projects. Given that the objective was to ensure the barrier would not be unduly sensitive to uncertainties and would

not collapse under certain plausible adverse situations whilst avoiding an unduly conservative design, the corresponding structural capacity assessment was based on a minimum factor of safety of unity whilst its serviceability (i.e. deformation and retention capacity) was not checked under the robustness checking scenarios.

Table 4. Summary of cases for robustness checking in the design of FBS04a and their rationale.

| Robustness case | Description | Rationale |
|---|---|---|
| 1 | Extra impact phase after the design three load phases resulting in debris overtopping the flexible barrier | Uncertainty in both debris "fill up" mechanism and barrier deflection responses |
| 2 | Malfunctioning of energy-dissipating devices: allowable elongation of all devices being reduced by 50% | Uncertainty in the as-built quality of the devices, influences of corrosion and debris impact on the devices that may result in reduced allowable elongation |
| 3 | Malfunctioning of energy-dissipating devices: removal of a wire rope and the connected energy-dissipating devices from both layers of bottom and middle ropes | Energy-dissipating devices laid close to ground surface may be more vulnerable to corrosion and debris impact |

The results of the robustness checks are summarised in Table 5. For case 1, the effect of debris overtopping the flexible barrier was assessed. As the resulting additional drag force on the top ropes and the increased static earth pressure on the barrier were much smaller than the dynamic impact load, the barrier responses remained largely the same as the original design case. In comparison, the effects of malfunctioning of energy-dissipating devices were more notable. In case 2, the allowable elongation of all energy-dissipating devices was reduced by half. This resulted in complete utilisation of all devices in the lower bound case. As the wire ropes mobilised their own stiffness, the developed cable forces were increased by over 30%. Over-utilisation of the energy-dissipating devices was not a concern in the robustness check as long as the wire ropes did not break. Case 3 assumed a pair of energy-dissipating devices in the bottom and middle ropes to be completely malfunctioned. This led to a significant increase in the rope forces. Hence, a robust design should provide extra redundancy to the wire ropes, especially those envisaged to be subject to the main debris impact.

Table 5. Summary of the results of robustness check for FBS04a.

| | Maximum axial force per rope (kN)[utilisation ratio shown in bracket] | | | |
|---|---|---|---|---|
| | **Design case** | **Robustness case 1** | **Robustness case 2** | **Robustness case 3** |
| Lower bound case | 160[100%] | 160[100%] | 215[130%] | 231[110%] |
| Upper bound case | 220[46%] | 220[46%] | 220[92%] | 263[64%] |

## 5. Suggestions on configuring a valley-shaped flexible barrier

Based on the insights gained from this study, some suggestions on configuring a valley-shaped flexible barrier for use in a drainage line or incised topography are given below.

- The flexible barrier should be aimed to fit in the drainage line with a view to avoiding unnecessary modification of the channel. Topographic survey at the envisaged barrier location at an early stage would be beneficial to the design.

- The overall barrier size is controlled by its retention capacity, which is established based on the deflected barrier height as estimated from the structural analysis, and whether debris overflow is allowed for or not.

- The wire rope layout of a valley-shaped flexible barrier typically comprises the bottom, top, border and winglet ropes (Figure 5). They are to be anchored directly to the channel sides. If the lateral span is excessive, steel posts on hinged base tied by the retain ropes should be provided. As a reference, Volkwein [19] suggested 15 m–20 m as the limiting span.

- The provision of middle wire ropes should be designed on a case-by-case basis. These serve to provide extra restraint to limit the barrier deflection and directly share part of the debris impact load. The effects of including middle ropes are illustrated in Figure 12 based on the design of FBS04a as discussed above. The utilisation ratios of energy-dissipating devices are compared between the original barrier configuration (i.e. with two layers of middle ropes) and that modified by omitting only the lower layer or all the middle ropes. It transpired that the absence of middle ropes would result in over-utilisation of almost all energy-dissipating devices. While incorporating the upper middle ropes could only relieve the forces induced in the top and winglet ropes, the additional lower middle ropes were able to reduce the forces induced in other ropes. In any event, the middle ropes should be strategically positioned in localities where the impact is expected to be the most intense (usually the lower portion of the barrier).

- All wire ropes should be equipped with sufficient energy-dissipating devices. For the longitudinal support ropes, they can be specified in pairs (i.e. in series) so as to offer extra flexibility for the barrier to deflect. Where extra stiffness is deemed necessary to restrain the barrier deflection, the energy-dissipating devices can be placed in parallel. They are specified in terms of the force-elongation characteristic curve. Unless a certain proprietary product is aimed at, the lower and upper bound design curves similar to the ones shown in Figure 6 may be specified.

- The number and size of wire ropes should be determined based on a detailed structural analysis of the flexible barrier subject to debris impact loading. The barrier configuration should be revised after reviewing the results of structural analysis in order to achieve better optimisation under the

prescribed design requirements. The utilisation ratio of energy-dissipating devices (Equation (3)) serves as an appropriate index to gauge the degree of design optimisation.

- The structural analysis may be conducted based on the pseudo-static approach as presented in this study. Such an analysis, however, does not properly cater for the dynamic effect of an impact, and thus might over-estimate the cable forces giving conservative solutions. Coupled analysis that explicitly takes into account the debris–barrier interaction (as introduced by Kwan et al. [27]) may yield further design optimisation.

Figure 12. Effects of varying the number of layers of middle wire ropes on the utilisation of energy-dissipating devices.

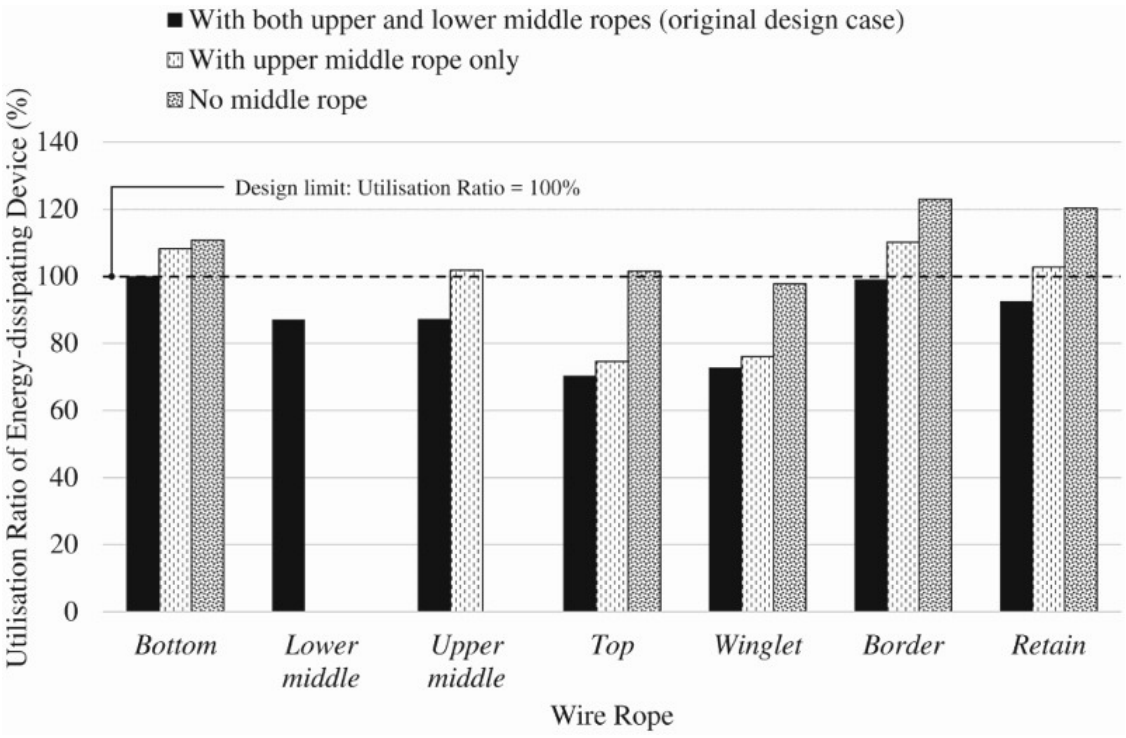


## 6. Concluding remarks

A new type of flexible debris-resisting barrier that is suitable for use in drainage lines against sizeable and mobile landslides such as channelised debris flow has been developed in a recent LPMitP project. Its layout is different from the conventional flexible barriers, rendering it geometrically more favourable and structurally more effective for the use in an incised topography. The design and analysis of this valley-shaped barrier, based on the state-of-the-art analytical force approach, has been presented in this paper. The use of the force approach has often been complicated by the need to pre-select a certain energy-dissipating device at the design stage to be commensurate with the design assumptions. In this project, this constraint was removed by introducing two bounding force-elongation

characteristic design curves for modelling the limiting behaviours of the flexible barriers. In addition, the concept of a robustness check has been introduced to examine the barrier performance under certain adverse scenarios. This is particularly important given the present understanding of the flexible barrier behaviour under debris impact is still limited. Based on the findings and insight from this study, some suggestions on how to better configure a valley-shaped flexible barrier are made for consideration by practitioners.

## Acknowledgements

This paper is published with the permission of the Head of the Geotechnical Engineering Office, the Director of Civil Engineering and Development, and Architectural Services Department, the HKSAR Government.

## References

1. Roth A, Kästli A, Frenez T. Debris flow mitigation by means of flexible barriers. Proceedings of the 10th International Congress INTERPRAEVENT, Riva del Garda; 26 May 2004; Klagenfurt: INTERPRAEVENT.

2. Wendeler C, McArdell BW, Rickenmann D, et al. Field testing and numerical modelling of flexible debris flow barriers. Proceedings of the International Conference on Physical Modelling in Geotechnics, Hong Kong; 2006.

3. Kwan JSH, Chan SL, Cheuk JCY, et al. A case study on an open hillside landslide impacting on a flexible rockfall barrier at Jordan valley, Hong Kong. Landslides. 2014;11(6):1037–1050. doi: 10.1007/s10346-013-0461-x

4. European Organisation for Technical Approvals. Guideline for European technical approval of falling rock protection kits – ETAG 027. European Organisation for Technical Approvals; 2013. p. 59.

5. Grassl H, Bartelt PA, Volkwein A, et al. Experimental and numerical modeling of highly flexible rockfall protection barriers. In: Culligan P, Einstein HH, Whittle AJ, editors, Proc. soil and rock America. Cambridge (MA): Verlag Glückauf, Essen; 2003. p. 2589–2594.

6. Bugnion L, Denk M, Shimojo K, et al. Full-scale experiments on shallow landslides in combination with flexible protection barriers. In: Proceedings of 1st world landslide forum; Tokyo, Japan; 2008. p. 99–102.

7. Roth A, Wendeler C, Amend F. Use of properly designed flexible barriers to mitigate debris flow natural hazards. Proceedings of GeoFlorida; Orlando, Florida, the United States; 2010.

8. Volkwein A, Wendeler C, Guasti G. Design of flexible debris flow barriers. Proceedings of the 5th International Conference on Debris-flow Hazards Mitigation,

Mechanics, Prediction and Assessment; Padua, Italy; 2011.

9. Geotechnical Engineering Office. Guidelines on empirical design of flexible barriers for mitigating natural terrain open hillside landslide hazards, GEO Technical Guidance Note No. 37. Geotechnical Engineering Office, the HKSAR Government; 2014. p. 18.

10. Kwan JSH, Cheung RWM. Suggestions on design approaches for flexible debris-resisting barriers, GEO Discussion Note 1/2012. Geotechnical Engineering Office, the HKSAR Government; 2012. p. 91.

11. Ng AKL, Williamson SJ, Chong AKT. Developments in design considerations and use of flexible barriers as mitigation measures for channelised debris flow and open hillslope failures – A case study. Proceedings of the One Day Seminar on Natural Terrain Hazard Mitigation Measures; Hong Kong; 2012. p. 61–66.

12. Chan SL, Zhou ZH, Liu YP, et al. Green structures and construction for natural terrain protection in Hong Kong by innovative flexible barrier design. Proceedings of the Joint Structural Division Annual Seminar; Hong Kong; 2017. p. 130–147.

13. Ho HY, Roberts KJ. Guidelines for natural terrain hazard studies, GEO Report No. 138 (Second Edition). Geotechnical Engineering Office, the HKSAR Government; 2016. p. 176.

14. Hungr O. A model for the runout analysis of rapid flow slides, debris flows, and avalanches. Canadian Geotechnical Journal. 1995;32(4):610–623. doi: 10.1139/t95-063

15. Geotechnical Engineering Office. Guidelines on the assessment of debris mobility for channelised debris flows, GEO Technical Guidance Note No. 29. Geotechnical Engineering Office, the HKSAR Government; 2011. p. 6.

16. Geotechnical Engineering Office. Guidelines on the assessment of debris mobility for open hillslope failures, GEO Technical Guidance Note No. 34. Geotechnical Engineering Office, the HKSAR Government; 2012. p. 16.

17. Geotechnical Engineering Office. Guidelines on the assessment of debris mobility for failures within topographic depression catchments, GEO Technical Guidance Note No. 38. Geotechnical Engineering Office, the HKSAR Government; 2013. p. 8.

18. Sun HW, Law RPH. A preliminary study on impact of landslide debris on flexible barriers, GEO Report No. 309. Geotechnical Engineering Office, the HKSAR Government; 2015. p. 50.

19. Volkwein A. Numerische simulation von flexiblen Steinschlagschutzsystemen. 2014. Doktorarbeit, Eid-genossishe Technische Hochschule Zurich.

20. Chan SL, Zhou ZH, Liu YP. Numerical analysis and design of flexible barriers allowing for sliding nodes and large deflection effects. Proceedings of the One Day Seminar on Natural Terrain Hazards Mitigation Measures; Hong Kong; 2012. p. 29–43.

21. Volkwein A. Flexible debris flow barriers – design and application. WSL Ber. 18; 2014. p. 29.

22. Koo RCH, Kwan JSH, Lam C, et al. Dynamic response of flexible rockfall barriers under different loading geometries. Landslides. 2017;14(3):905–916. doi: 10.1007/s10346-016-0772-9

23. Geotechnical Engineering Office. Assessment of landslide debris impact velocity for design of debris-resisting barriers, GEO Technical Guidance Note No. 44. Geotechnical Engineering Office, the HKSAR Government; 2015. p. 4.

24. Koo RCH, Kwan JSH, Ng CWW, et al. Velocity attenuation of debris flows and a new momentum-based load model for rigid barriers. Landslides. 2017;14(2):617–629. doi: 10.1007/s10346-016-0715-5

25. Huang Y, Yiu J, Pappin JW, et al. Numerical investigation of landslide mobility and debris-resistant flexible barrier with LS-DYNA. In: Proceedings of the 13th International LS-DYNA Users Conference; 8-10 June 2014; Dearborn, Livermore; Livermore Software Technology Corporation; 2014.

26. Bartelt P, Volkwein A, Wendeler C. Full-scale testing and dimensioning of flexible debris flow barriers. Summary Report CTI Debris Flows. Swiss Federal Institute of Forest, Snow and Landscape Research; 2009. p. 22.

27. Kwan JSH, Koo RCH, Law RPH, et al. Discussion: trends in large-deformation analysis of landslide mass movements with particular emphasis on the material point method. Géotechnique, published online ahead of print; 2018.